JOURNAL OF SOLID STATE CHEMISTRY 90, 185–193 (1991)

Structure and Thermal Expansion of $LiGe_2(PO_4)_3$

M. ALAMI AND R. BROCHU

Département de Chimie de la Faculté des Sciences de l'Université Mohamed V, Avenue Ibn Batouta, Rabat, Maroc

J. L. SOUBEYROUX

Institut Laüe-Langevin, Avenue des Martyrs 156 ×, 38042 Grenoble Cedex, France

AND P. GRAVEREAU, G. LE FLEM, AND P. HAGENMULLER

Laboratoire de Chimie du Solide du CNRS, 351 cours de la Libération, 33405 Talence Cedex, France

Received April 9, 1990; in revised form August 1, 1990

$LiGe_2(PO_4)_3$ belongs to the Nasicon-type family. Room-temperature structure has been determined on a single crystal from 3D X-ray data. Thermal evolution of this structure has been established from neutron powder diffraction data between 300 and 1000 K using the Rietveld method. The thermal expansion is positive along the *c*-axis, whereas shrinking is observed along the *a*-axis below 900 K, followed by dilatation. The atomic displacements noted with increasing temperature are consistent with a model proposed for $NaZr_2(PO_4)_3$. © 1991 Academic Press, Inc.

The $LiGe_2(PO_4)_3$ phosphate may occur both in crystalline state and in vitreous state (*1*). The crystallized species has Nasicon-type structure. Several members of this structural family are near zero thermal expansion materials and have industrial applications (*2–4*). The existence of a glass of similar composition opened the possibility of elaborating a low-thermal expansion glass-ceramic.

In this general scope the present investigation covers:

(i) crystal structure determination of $LiGe_2(PO_4)_3$ from X-ray single crystal data, and

(ii) thermal expansion investigation of the ceramic by neutron diffraction structure analysis between room temperature and 1000 K.

Crystal Structure of $LiGe_2(PO_4)_3$ at Room Temperature from X-Ray Diffraction

Single crystals of $LiGe_2(PO_4)_3$ were obtained by a flux technique; the germanium oxide is dissolved in an excess of $LiPO_3$ with respect to following reaction:

$$5LiPO_3 + 2GeO_2 \rightarrow LiGe_2(PO_4)_3 + Li_4P_2O_7.$$

The mixture was heated in air for several hours at 1050°C and then cooled at a rate of

0022-4596/91 $3.00

TABLE I

CONDITIONS USED FOR DATA COLLECTION OF $LiGe_2(PO_4)_3$ SINGLE CRYSTAL

Radiation	Mo$K\alpha$ (graphite monochromatized) $\lambda = 0.7107$ Å
$T = 20$°C	
Scanning	ω
Angular range	$0.1 < \theta < 35°$
hkl limits of the explored reciprocal space	$-13 \leq h \leq 12$ $-13 \leq k \leq 13$ $-13 \leq l \leq 32$
Scanning width counter slit width	$0.86 + 0.44 \tan \theta$ (°) $0.09 + 0.21 \tan \theta$ (mm)
Total number of measured reflections	3.472
Independent data $F_o^2 > 3\,\sigma\,(F_o^2)$: 527	

$$R_{INT} = \frac{\Sigma\Sigma[F_o - \langle F_o \rangle]}{\Sigma F_o} = 0.031$$

Note. The data were corrected for Lorentz-polarization effects but not for absorption ($\mu_R = 0.8$).

5°C hr^{-1} down to 400°C. Single crystals were extracted by removing the lithium diphosphate with hot water.

The crystallographic investigation was carried out on a crystal of parallelepipedic shape (120 × 190 × 220 μm). The Laue photographs gave evidence of a trigonal symmetry. Systematic absences

$$(hkl): -h + k + l \neq 3n$$
$$(hhl): h + l \neq 3n; \quad l \neq 2n$$

are compatible with the $R\bar{3}c$ or $R3c$ space group.

The cell parameters were refined using 22 reflections from X-ray powder diffraction (the internal standard was Al), either

$$a_H = 8.275(5) \text{ Å}; \quad c_H = 20.47(3) \text{ Å},$$

or $a_R = 8.33$ Å; $\alpha_R = 59.6°$.

The measured specific mass (3.56 g cm^{-3}) is in good agreement with the calculated one (3.61 g cm^{-3} with $Z = 6$ in the hexagonal cell).

Data collection was achieved with an ENRAF-NONIUS CAD3 automatic diffractometer and with conditions given in Table I.

All calculations were made with the SHELX 76 (*5*) program in the $R\bar{3}c$ space group. Atomic scattering factors and anomalous dispersion corrections were taken from "International Tables for X-Ray Crystallography" (*6*).

All nonlithium atoms were located using the $NaZr_2(PO_4)_3$ structure as a model (*7*). In those conditions, assuming individual isotropic thermal parameters for all atoms, the *R* factor was 0.12. A difference Fourier synthesis revealed a residual peak at the origin, i.e., at the M_1 site (6b). There is no significant electron density near the second possible site, i.e., M_2 (18e) (*20*).

Calculations were carried out assuming the lithium ions to be distributed over both M_1 and M_2 sites with a refinement of the correlated occupation factors. They confirm only occupancy of the M_1 site.

A final calculation was achieved with lithium ions at the origin (site M_1), but now using individual anisotropic thermal parameters for all atoms, a weighting factor $w = 1/\sigma 2\,(F_o)$ and an empirical isotropic extinc-

TABLE II

ATOMIC PARAMETERS OF $LiGe_2(PO_4)_3$

Atoms	Position	Site symmetry	x	y	z	Beq(A)^2
Li	6b	$\bar{3}$.	0	0	0	2.44
Ge	12c	3.	0	0	0.14097(1)	0.26
P	18e	.2	0.2879(1)	0	$\frac{1}{4}$	0.28
O_1	36f	1	0.1802(2)	−0.0152(2)	0.1883(1)	0.85
O_2	36f	1	0.1845(2)	0.1593(2)	0.0821(1)	0.65
			$\times 10^4$ (Å)^2			
	U_{11}	U_{22}	U_{33}	U_{23}	U_{13}	U_{12}
Li	405(50)	U_{22}	118(45)	0	0	$U_{11}/2$
Ge	30(1)	U_{11}	37(2)	0	0	$U_{11}/2$
P	26(2)	34(3)	49(3)	12(2)	$U_{23}/2$	$U_{23}/2$
O_1	103(6)	138(7)	106(6)	6(5)	−45(5)	77(5)
O_2	52(5)	65(6)	81(5)	10(5)	10(4)	−8(5)

Note. Atomic coordinates and equivalent isotropic parameters for $LiGe_2(PO_4)_3$ (Beq $= (8\pi^2/3)\sum_{i=1}^{i=3}\sum_{j=1}^{j=3} a^*_i a^*_j U_{ij}(\mathbf{a}_i \cdot \mathbf{a}_j)$).

U_{ij} coefficients of anisotropic thermal parameters. $T = \exp -2\pi^2(h^2a^{*2}U_{11} + k^2b^{*2}U_{22} + l^2c^{*2}U_{33} + 2hka^*b^*U_{12} + 2hla^*c^*U_{13} + 2klb^*c^*U_{23})$.

tion parameter x ($F_c = F(1-10^{-4} \cdot x \cdot F^2/\sin\theta)$). It converged down to $x = 0.0029(1)$, with $R = 0.0239$ and $R_w = 0.0236$. The obtained atomic parameters are given in Table II.

TABLE III

INTERATOMIC ANGLES AND DISTANCES IN $LiGe_2(PO_4)_3$ (ROOM TEMPERATURE AND X-RAY DIFFRACTION DATA)

Li–O_2: 6 × 2.210(1) (Å)	O_2–Li–O_2i: 68.4(0.1)°
Ge–O_1: 3 × 1.834(1) (Å)	O_1–Ge–O_1i: 94.7(0.1)°
	O_1–Ge–O_2: 89.0(0.1)°
Ge–O_2: 3 × 1.872(1) (Å)	O_1–Ge–O_2i: 171.5(0.1)°
	O_1–Ge–O_2ii: 92.6(0.1)°
	O_2–Ge–O_2i: 83.1(0.1)°
P–O_1: 2 × 1.515(1) (Å)	O_1–P–O_1iv: 113.7(0.1)°
	O_1–P–O_1iii: 112.9(0.1)°
P–O_2*iii*: 2 × 1.530(1) (Å)	O_1–P–O_2v: 104.2(0.1)°
	O_2iii–P–O_2v: 109.1 (0.1)°

Note. Symmetry operation codes: i, $-y, x-y, z$; ii, $y-x, -x, z$; iii, $\frac{2}{3}-x, \frac{1}{3}-y, \frac{1}{3}-z$; iv, $x-y, -y, \frac{1}{2}-z$; v, $\frac{1}{3}+y-x, -\frac{1}{3}+y, -\frac{1}{3}+\frac{1}{2}+z$.

The thermal motion of lithium exhibits a relatively strong anisotropic character with greater displacements in the (a, b) plane than along the c-axis. This anisotropy in the M_1 site is in good agreement with the Nasicon lattice model. The Beq parameter has a reasonable value (2.44 Å^2). In addition calculations involving a Li^+ ion-delocalization in the plane (a, b) near the origin lead to a nonsignificant weak value of x, strongly correlated with thermal parameters.

The interatomic distances and angles calculated for $LiGe_2(PO_4)_3$ from the X-ray diffraction data are given in Table III.

Crystal Structure of $LiGe_2(PO_4)_3$ Determined by Neutron Diffraction Investigation

The powder of $LiGe_2(PO_4)_3$ was prepared as previously described (*1*).

The neutron diffraction patterns were collected at ILL with the powder diffractometers D_{1A} (room temperature) and D_{1B} (300–1000 K). The neutron diffraction data

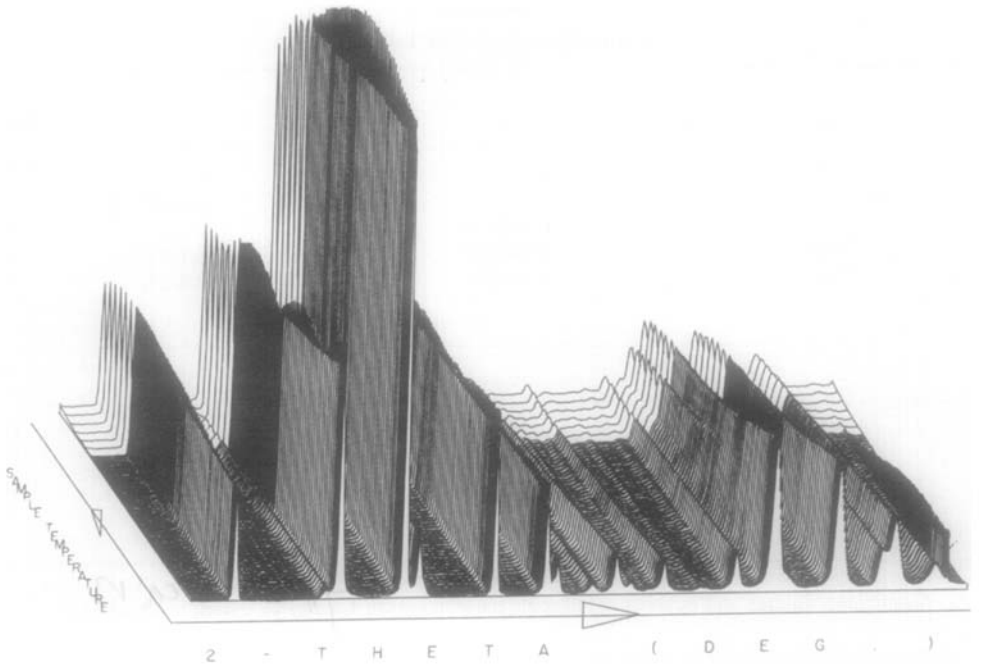

FIG. 1. Neutron diffraction patterns of $LiGe_2(PO_4)_3$ between 300 and 1000 K.

have been analyzed by the Rietveld profile method (*8*).

As the neutron diffractograms revealed the existence of GeO_2 as a minor parasitic phase, we utilized a refinement program allowing us to calculate simultaneously the parameters and intensities of both phases.

A tridimensional projection of the thermodiffractograms between 295 and 1000 K is given in Fig. 1.

About 80 structure determinations were carried out within this temperature range. Refinements converged to atomic positions very close to those found by X-ray diffraction except in the description of the Li^+ site. For lithium located in the (0,0,0) site the isotropic thermal factor is $B = 2.6$ Å^2. Lowering R supposes a lithium shift to an off-centered position in the basal (a, b) plane (with a large standard deviation) and a related decrease of B

All previously reported results concerning the structure either of $LiTi_2(PO_4)_3$ (*9*) or of $LiZr_2(PO_4)_3$ (*10*) gave evidence of the highly anisotropic character of the thermal parameters associated with the lithium position in the (a, b) plane.

Table IV compares the final atomic coordinates obtained at 300 K by both X-ray and neutron diffraction techniques.

In the following discussion we shall assume the lithium ions to have average 0,0,0 coordinates similar to those of $LiTi_2(PO_4)_3$ or $LiZr_2(PO_4)_3$.

Figure 2 shows the thermal expansion of the crystal lattice of $LiGe_2(PO_4)_3$ between 300 and 1000 K and the corresponding mean thermal expansion coefficients $\langle\alpha\rangle$

At high temperature $LiGe_2(PO_4)_3$ remains trigonal. At rising temperature the c-parameter increases, whereas the a-parameter decreases between 300 and 900 K and then increases.

Phosphorus, zirconium, and oxygen keep the same positions in the investigated temperature range. Examples of evolution of

TABLE IV

ATOMIC PARAMETERS OF $LiGe_2(PO_4)_3$

	Neutrons λ = 1.912 Å N_{hkl} = 140	Neutrons λ = 2.524 Å N_{hkl} = 32	X-ray λ = 0.7107 Å N_{hkl} = 527
a(Å)	8.2722(2)	8.2682(9)	8.272(5)
c(Å)	20.4825(7)	20.494(4)	20.47(3)
Li_1			
x	0.025(2)	0.025	0
y	0	0	0
z	0	0	0
B(Å)^2	1.3(6)	0.9(3)	2.44
Ge			
x	0	0	0
y	0	0	0
z	0.1412(1)	0.1403(8)	0.14097(1)
B(Å)^2	0.84(7)	0.5(3)	0.26
P			
x	0.2867(5)	0.288(4)	0.2879(1)
y	0	0	0
z	1/4	1/4	1/4
B(Å)^2	0.72(8)	1.7(4)	0.28
O_1			
x	0.1786(4)	0.182(2)	0.1802(2)
y	0.98278(4)	0.985(2)	0.9848(2)
z	0.1888(1)	0.1894(6)	0.1883(1)
B(Å)^2	1.60(7)	1.8(5)	0.85
O_2			
x	0.1849(3)	0.186(1)	0.1845(2)
y	0.1595(3)	0.160(2)	0.1593(2)
z	0.0829(1)	0.0826(6)	0.0821(1)
B(Å)^2	0.93(6)	0.5(2)	0.65
R_I %	5.5	3.8	R % 2.4
R_W %	6.9	4.8	R_W % 2.4

some interatomic angles and distances obtained from Rietveld refinements are given in Table V.

Structure Description

The structure of $LiGe_2(PO_4)_3$ consists of a three-dimensional framework of PO_4 tetrahedra and GeO_6 octahedra sharing common corners. As emphasized before, lithium ions occupy only the M_1 site which is a trigonal antiprism elongated along the c-axis (Fig. 3).

The Ge–O distances of the distorted GeO_6 octahedra (1.834 and 1.872 Å) are equal to or shorter than the values reported for GeO_2 of rutile-type structure: 1.872 and 1.902 Å (*11*).

The PO_4 tetrahedra are rather regular with a weak angular dispersion of the O–P–O angles between 104.2 and 113.8° around the ideal value of 109.45°. The P–O_1 and P–O_2 distances have an average value of 1.525 Å, which is close to the P–O distances found for $LiTi_2(PO_4)_3$ (1.530 Å) (*9*), $LiZr_2(PO_4)_3$ (1.522 Å) (*10*), or $NaZr_2(PO_4)_3$ (1.543 Å) (*7*).

Assuming the lithium atoms to be located at the center of the M_1 site, the Li–O distance (2.210 Å) is very close to that expected from Shannon's table (2.16 Å) (*17*) but significantly lower than those found for Li $Ti_2(PO_4)_3$ [2.26 Å (*9*)] and even more so for $LiZr_2(PO_4)_3$ [2.491 Å (*10*)]. All these values are consistent with the increasing c-parameter: 20.88 Å (Ti) and 22.24 Å (Zr).

Thermal Structure Evolution of $LiGe_2(PO_4)_3$

Between 300 and 1000 K the Ge–O distances remain remarkably constant but both P–O_1 and P–O_2 distances reach progressively the same value (1.5075 Å) at 900 K

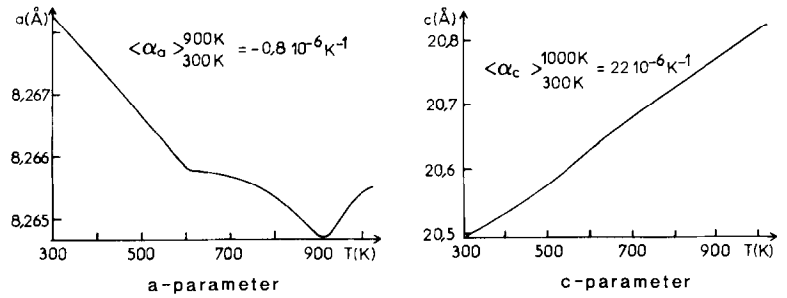

FIG. 2. Thermal expansion of the a- and c-parameters of $LiGe_2(PO_4)_3$ between 300 and 1000 K.

TABLE V

THERMAL EVOLUTION OF $LiGe_2(PO_4)_3$: Interatomic Angles and Distances

	300 K	400 K	600 K	800 K	900 K	1000 K
Distances(R)						
P–O_1	1.498(1)	1.496(3)	1.502(7)	1.504(2)	1.506(3)	1.517(2)
P–O_2	1.527(5)	1.527(1)	1.516(1)	1.512(8)	1.507(8)	1.5175
⟨P–O⟩	1.5125	1.5117	1.5094	1.5085	1.5071	1.5173
Ge–O_1	1.849(7)	1.847(9)	1.849(2)	1.848(6)	1.847(2)	1.839(1)
Ge–O_2	1.865(2)	1.870(1)	1.862(7)	1.865(6)	1.870(1)	1.855(6)
⟨Ge–O⟩	1.8575	1.859	1.856	1.857	1.858	1.847
⟨Li–O⟩	2.210	2.234	2.257	2.274	2.288	2.285
Angles(°)						
O_1–P–O_1	113.50	113.9	110.13	108.94	108.37	107.18
O_2–P–O_2	109.44	109.65	112.83	114.13	114.12	114.44
O_1–P–O_2	104.34	104.27	104.84	105.09	104.90	105.02
O_1–P–O_2	112.69	112.65	112.16	112.00	112.27	112.36

and then increase. The mean ⟨Li–O⟩ distance increases also between 300 and 900 K and then remains constant. A similar evolution had been observed for $NaZr_2(PO_4)_3$ (*19*).

The flexibility of the $M(IV)_2(PO)_3$ skeleton allows a rotation of the oxygen atoms around the c-axis at the M_1 site, alternatively clockwise and counterclockwise, involving a rotation of the PO_4 groups schematized in Fig. 4.

All these displacements result in an elongation of the M_1 antiprism along the c-axis.

A mechanism for such thermal behavior was postulated by Lenain *et al.* (*13*). The shifts of both polyhedra can be described by a projection of the $|MO_6|$ octahedron onto the plane perpendicular to the c-axis and a

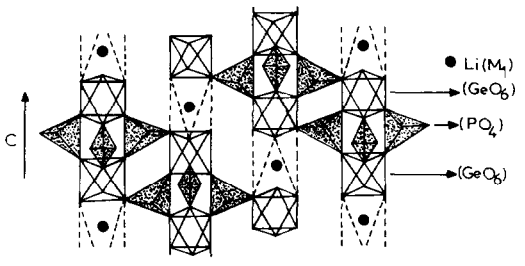

FIG. 3. Schematic drawing of the skeleton of the $LiGe_2(PO_4)_3$.

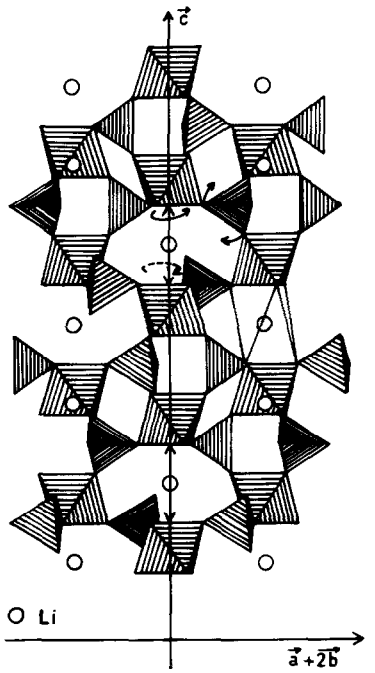

FIG. 4. Mechanism of the thermal expansion of $LiGe_2(PO_4)_3$.

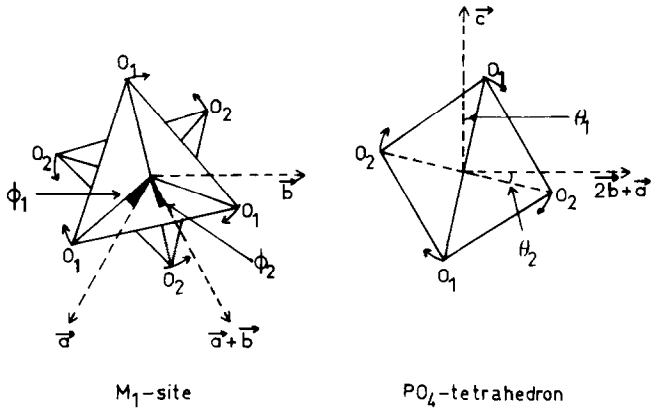

FIG. 5. Oxygen displacement around the M_1 site and for the PO_4 tetrahedron (according to Lenain *et al.* (13)).

projection of the PO_4 tetrahedron onto the plane perpendicular to the a-axis. The movements of oxygen are characterized by the ϕ_1 and θ_1 angles for O_1, and ϕ_2 and θ_2 for O_2, which are defined in Fig. 5.

The results collected in Table VI show clearly that O_1 shifts more than O_2 in agreement with the previous variations reported in $NaTi_2(PO_4)_3$ (*15*) and $NaZr_2(PO_4)_3$ (*19*).

Owing to the similarity of the mechanism shown for thermal expansion in such materials, it was worthwhile to relate the thermal expansion coefficients to the structural parameters of the phases at room temperature in order to show that the thermal behavior could be predicted from the structural information.

Conclusion: The Thermal Expansion of Nasicon-Type Phosphates $M(I)$ $M(IV)_2$ $(PO_4)_3$

The relations between the crystal structure of $NaZr_2(PO_4)_3$-type compounds and the thermal expansion have been investigated previously by several authors (*12–16, 19, 21*). In the present discussion are mentioned only the results concerning phosphates with composition $M(I)$ $M(IV)_2$ $(PO_4)_3$, where the monovalent ions are lo-

TABLE VI

APPLICATION OF LENAIN'S MODEL (*13*) TO THE THERMAL EXPANSION OF $LiGe_2(PO_4)_3$: THERMAL EVOLUTION OF THE INTERNAL PARAMETERS

	300 K	400 K	600 K	800 K	900 K	1000 K
$\theta_1°$	5.01	5.22	5.80	6.34	6.70	7.00
$\theta_2°$	0.94	0.60	0.70	1.30	1.56	2.02
$\theta_1-\theta_2°$	4.07	4.62	5.11	5.04	5.14	4.98
$\phi_1°$	4.11	4.24	4.60	5.00	5.29	5.61
$\phi_2°$	7.53	7.70	8.28	8.86	8.55	8.26
$\phi_2-\phi_1°$	3.42	3.46	3.68	3.66	3.26	2.65

TABLE VII

CELL PARAMETERS AND AVERAGE INTERATOMIC DISTANCES OF VARIOUS NASICON-TYPE PHOSPHATES: $M(I)\ [M(IV)]_2(PO_4)_3$

	⟨P–O⟩ (Å)	⟨M(IV)–⟩ (Å)	⟨M(I)–O⟩ (Å)
$LiTi_2(PO_4)_3$ (*9*)	1.530	1.930	2.260
a = 8.52 ?A			
c = 20.88 Å			
$NaTi_2(PO_4)_3$ (*15*)	1.510	1.948	2.472
a = 8.4876 Å			
c = 21.801 Å			
$LiZr_2(PO_4)_3$ (*10*)	1.522	2.061	2.499
a = 8.847 Å			
c = 22.243 Å			
$NaZr_2(PO_4)_3$ (*7*)	1.531	2.066	2.538
a = 8.8043 Å			
c = 22.7585 Å			
$KZr_2(PO_4)_3$ (*18*)	1.522	2.063	2.813
a = 8.71 Å			
c = 23.89 Å			

cated in the M_1 site. The cell parameters are obtained and mean interatomic distances are summarized in Table VII for phosphates whose detailed structural determinations have been published.

The thermal expansion coefficients are given in Tables VIII and IX as far as they are known.

The ⟨P–O⟩ and ⟨M(IV)–O⟩ distances are quite constant [they are close to the values given in Shannon's table (*17*)]. The c-parameters are influenced by the size of the $M(I)$ cations and the thermal expansion along the c-axis α_c is connected to the stretching of the MO_6 antiprism: a wide $M(I)$ size brings about a larger stretching expansion already at room temperature and a lower α_c. Such a trend was qualitatively observed in (*16, 19*) for the $MZr_2(PO_4)_3$ (M = Li, Na, K) phosphates.

At room temperature, for a given $M(IV)$ element a decreases as the ionic radius of $M(I)$ increases. In correlation, the thermal expansion of the M_1 site gives rise to contraction of the cell in a direction perpendicular to the c-axis and the expansion coefficient along the a-axis becomes negative. This shrinkage is limited by the distortion possibility of the strongly covalent PO_4 groups and their ability to move. Obviously a limitation of such an evolution will be quickly attained for compounds with a relatively low a-parameter such as $LiGe_2(PO_4)_3$.

A very simple model can account for the α_a and α_c values found for $LiGe_2(PO_4)_3$. Since the ⟨M(IV)–O⟩ distances are practically temperature independent the tensions along the c-axis can be characterized by the ⟨M(IV)–O⟩ distance over the c-parameter ratio (labeled as δ) and along the a-axis by the ⟨M(IV)–O⟩ distance over the a-parame-

TABLE VIII

$\langle\alpha_c\rangle$ (K^{-1}) AND δ PARAMETERS OF VARIOUS NASICON-TYPE PHOSPHATES $M(I)[M(IV)]_2(PO_4)_3$ (SEE TEXT)

Phosphates	$10^6\alpha_c$ (K^{-1})	10^2
$LiZr_2(PO_4)_3$ (*16*)	24	9.27
$LiZr_2(PO_4)_3$ (*21*)	28.9	9.32
$NaZr_2(PO_4)_3$ (*16*)	23	9.08
$LiZr_2(PO_4)_3$ (*19*)	22.4	
$LiGe_2(PO_4)_3$	22	9.05
$NaTi_2(PO_4)_3$ (*15*)	21.3	8.93
$KZr_2(PO_4)_3$ (*13, 16*)	0	8.63

TABLE IX

$\langle a_a \rangle$ (K^{-1}) AND γ PARAMETERS OF VARIOUS NASICON-TYPE PHOSPHATES $M(I)[M(IV)]_2(PO_4)_3$ (SEE TEXT)

Phosphates	$10^6 \langle \alpha_a \rangle$ (K^{-1})	γ
$LiZr_2(PO_4)_3$ (*16*)	−10	0.2330
$LiZr_2(PO_4)_3$ (*21*)	−5.53	0.2329
$NaZr_2(PO_4)_3$ (*16*)	−6.4	0.2346
$LiZr_2(PO_4)_3$ (*19*)	−5.4	
$KZr_2(PO_4)_3$ (*16, 13*)	−5	0.2368
$NaTi_2(PO_4)_3$ (*15*)	−4.45	0.2295
$LiGe_2(PO_4)_3$	−0.8	0.2240

ter ratio (i.e., γ). As the strains increase, α_c and δ increase and γ and α_a decrease. Table VIII and IX list the δ and γ values by considering only the $\langle M(IV)–O \rangle$ distances deduced from a detailed RT structure determination.

For a given $M(IV)$ (e.g., zirconium), a larger $M(I)$ size leads to a lower a-parameter, which becomes obviously less shrinkable. As a result $|\langle \alpha_a \rangle|$ becomes smaller. For a given $M(I)$ cation, as the size of $M(IV)$ decreases [e.g., $NaTi_2(PO_4)_3$ with respect to $NaZr_2(PO_4)_3$ or $LiGe_2(PO_4)_3$ compared to $LiZr_2(PO_4)_3$] a decreases as well as $|\langle \alpha_a \rangle|$.

The behavior of $LiGe_2(PO_4)_3$ can be understood as an extrapolation of both trends, leading to a small negative value of α_a, which becomes positive only at about 900 K.

Finally it is worthwhile to plot γ against $f(M(IV)–O)$ for the lithium and sodium phosphates (Fig. 6).

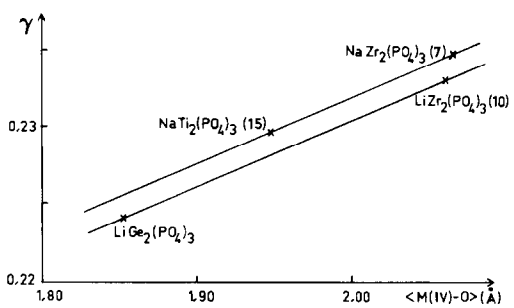

FIG. 6. Variation of γ versus $\langle M(IV)–O \rangle$ distances for various Nasicon-type phosphates (see text).

The two graphs are parallel, which confirms the similarity of the mechanism of internal adjustment observed for the structure.

Indeed such a comparison is only valid when the cationic distribution within the materials is not influenced by the elaboration process (*21*).

References

1. M. ALAMI, R. BROCHU, C. PARENT, AND G. LE FLEM, C. R. *Acad. Sci. Paris* **306**(II), 1349 (1988).
2. J. ALAMO, R. ROY, AND H. A. MC KINSTRY, *Bull. Amer. Ceram. Soc.* **61,** 333 (1982).
3. J. ALAMO AND R. ROY, *J. Amer. Ceram. Soc.* **67**(5), 78 (1984).
4. R. ROY, D. K. AGRAWAL, J. ALAMO, AND R. A. ROY, *Mater. Res. Bull.* **19,** 471 (1984).
5. G. M. SHELDRICK, "SHELX 76, Program for Crystal Structure Determination," Univ. of Cambridge, England (1976).
6. "International Tables for X-Ray Crystallography, IV," Kynoch Press, Birmingham (Present Distributor Kluwer Academic Publishers, Dordrecht) (1974).
7. L. O. HAGMAN AND P. KIERKEGAARD, *Acta Chem. Scand.* **22,** 1822 (1968).
8. H. M. RIETVELD, *Acta Crystallogr.* **20,** 508 (1966). H. M. RIETVELD, *Acta Crystallogr.* **22,** 151 (1967). H. M. RIETVELD, *J. Appl. Crystallogr.* **2,** 65 (1986).
9. C. DELMAS, personal communication.
10. D. PETIT, P. COLOBAM, G. COLLIN, AND J. P. BOILOT, *Mater. Res. Bull.* **21,** 365 (1986).
11. W. H. BAUR AND A. A. KAHN, *Acta. Crystallogr. Sect. B* **27,** 2133 (1971).
12. J. ALAMO AND R. ROY, *J. Mater. Sci.* **21,** 444 (1986).
13. G. E. LENAIN, H. A. MC KINSTRY, J. ALAMO, AND D. K. AGRAWAL, *J. Mater. Sci.* **22,** 17 (1987).
14. P. R. RUDOLF, A. CLEARFIELD, AND J. D. JORGENSEN, *J. Solid State Chem.* **72,** 100 (1988).
15. J. L. RODRIGO, P. CARASCO, AND J. ALAMO, *Mater. Res. Bull.* **24,** 611 (1989).
16. T. OOTA AND I. YAMAI, *J. Amer. Ceram. Soc.* **69,** 1 (1986).
17. R. D. SHANNON, *Acta Crystallogr. Sect. A.* **32,** 751 (1976).
18. M. SLUJKIC, B. MATKOVIC, AND B. PRODIC, *Z. Kristallogr.* **130,** 148 (1969).
19. R. M. HAZEN, L. W. FINGER, D. K. AGRAWAL, H. A. MC KINSTRY, AND A. J. PERROTA, *J. Mater. Res.* **2**(3), 329 (1987).
20. J. B. GOODENOUGH, H. Y. P. HONG, AND J. A. KAFALAS, *Mater. Res. Bull.* **11,** 203 (1976).
21. J. ALAMO AND J. L. RODRIGO, *Solid State Ionics* **32/33,** 70 (1989).